Journal of
Nanoscience and Nanotechnology
Vol. 11, 1417–1420, 2011

Wettability Control and Flow Regulation Using a Nanostructure-Embedded Surface

Ehsan Yakhshi Tafti[1], Ghanashyam Londe[2], Anindarupa Chunder[3], Lei Zhai[3], Ranganathan Kumar[1], and Hyoung J. Cho[1, 4, *]

[1] *Department of Mechanical, Materials and Aerospace Engineering, University of Central Florida, Orlando, Florida, 32816, USA*
[2] *Department of Electrical Engineering, University of Central Florida, Orlando, Florida, 32816, USA*
[3] *Department of Chemistry and Nanoscience Technology Center, University of Central Florida, Orlando, Florida, 32816, USA*
[4] *School of Advanced Materials Science and Engineering, Sungkyunkwan University, Suwon 440-746, Korea*

This work addresses the synthesis, integration and characterization of a nanostructure-embedded thermoresponsive surface for flow regulation. In order to create a hierarchic structure which consists of microscale texture and nanoscale sub-texture, hybrid multilayers consisting of poly(allylamine hydrochloride) (PAH), poly(acrylic acid) (PAA) and colloidal silica nanoparticles (average diameter = 22 nm and 7 nm) were used. Based on the electrostatic interactions between the polyelectrolytes and nanoparticles, a layer-by-layer deposition technique in combination with photolithography was employed to obtain a localized, conformally-coated patch in a microchannel. Grafted with the thermoresponsive polymer, poly(N-isopropylacrylamide) (PNIPAAm), wettability of the surface could be tuned upon heating or cooling. The measurement of differential pressure at various stages of device verified the working conditions of the nanostructure-embedded surface for regulating a capillary flow in the microchannel.

Keywords: Wetting, Layer-by-Layer, Thermoresponsive Polymer, Valve.

RESEARCH ARTICLE

1. INTRODUCTION

Surfaces with tunable wettability can be used in applications such as flow regulation in microchannels,[1] force transduction,[2] drug delivery[3] and molecular filtering.[4] Surfaces functionalized with a thermally switchable polymer, poly(N-isopropylacrylamide) (PNIPAAm) can change their wettability responsive to changes in the ambient temperature. PNIPAAm has a lower critical solution temperature (LCST) range of about 28–33 °C. Below LCST, the polymeric chains extend and are hydrated giving rise to hydrophilic surface properties; while above the LCST range the polymer chains form intra-molecular hydrogen bonds and get dehydrated collapsing into compact hydrophobic structures.[5] However, the range of contact angle variation is limited between 60–90°. For practical applications, a wider range of tunability is desired.

As often found in nature, for example in a lotus leaf, many non-wetting surfaces consist of dual length scale structures, i.e., microscale texture and sub-texture at the smaller scale. Generally speaking, adding roughness to a surface accentuates its hydrophilic or hydrophobic properties; i.e., a rough surface of an inherently hydrophobic material has higher contact angle compared to a smooth surface of the same material and the same applies for hydrophilic surfaces.[6, 7] Therefore, PNIPAAm coatings together with appropriate surface roughness can provide surfaces with a wide range wettability; i.e., tunable-wetting surfaces ranging from superhydrophobic to superhydrophilic.[8] In this work, we fabricated a wettability control surface using nanostructure-embedded layers for flow regulation and tested its characteristics.

2. WORKING PRINCIPLE

The behavior of fluids at the reduced scale is highly influenced by factors such as surface tension, energy dissipation, quick thermal relaxation and fluidic resistance. Interfacial forces at solid–liquid–air contact lines gain significance and the characteristics of highly laminar regimes dominate fluid flow in microchannels. Water flows within the microchannel due to capillary action. For simplification, it is assumed that the velocity profile at any instance is given by the Poiseuille equation:[9]

$$u = \frac{dl}{dt} = \frac{r^2}{8\mu}\frac{p_{\text{in}} - p_{\text{m}}}{l} \quad (1)$$

*Author to whom correspondence should be addressed.

where l is the longitudinal coordinate along the channel and P_m is the capillary pressure at the advancing meniscus on the liquid side that drives (pulls) the flow inside the channel. By rearranging and integration, the following relationships are derived:

$$P_{in} - P_m = 4\mu\left(\frac{l}{r}\right)^2 \frac{1}{t} \tag{2}$$

The capillary pressure head resulting from the hydrophilic contact of water with glass is given by the Young-Laplace equation:

$$P_m - P_{atm} = -\frac{2\gamma \cdot \cos\theta}{r} \tag{3}$$

Elimination of P_m from Eqs. (2) and (3) results in:

$$P_{in} - P_{atm} = \Delta P = \frac{2\gamma\cos\theta}{r} - 4\mu\left(\frac{l}{r}\right)^2 \frac{1}{t} \tag{4}$$

Note that as long as the advancing front of the flow is in contact with the hydrophilic glass surface (low values of contact angle), favorable pressure gradient exists towards downstream (Fig. 1(a)), which is necessary to maintain the flow inside the capillary. However, when the advancing meniscus reaches the thermoresponsive surface (Fig. 1(b)), depending on the hydrophilic/hydrophobic state of the polymer surface, the contact angle between the liquid and the walls can change abruptly.

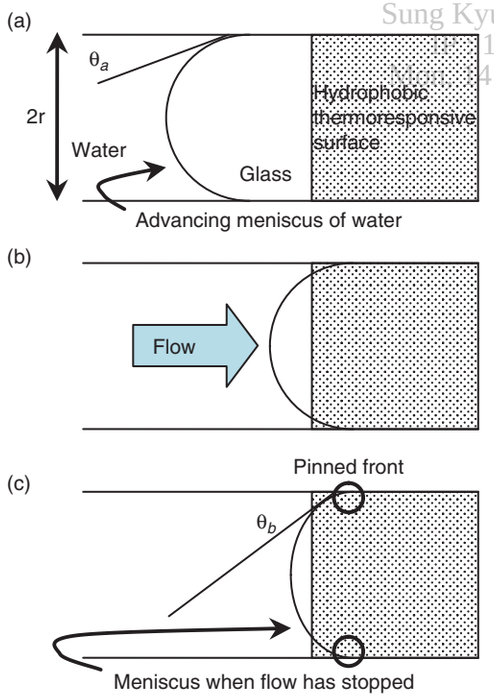

Fig. 1. (a) Meniscus advances due to concave interface and overall hydrophilic walls (small contact angle) (b) Advancing meniscus gets pinned to the hydrophobic surface. (c) The advancing meniscus of water after it has been stopped by the thermoresponsive hydrophobic surface. Larger contact angle prevents the meniscus from passing the valve ($\theta_a < \theta_b$).

In case the surface is in the hydrophobic mode (valve closed), the contact angle increases (fluid front becomes less concave) and the driving pressure gradient vanishes causing the flow to stop. By examining Eq. (4), it is expected that as the liquid enters and flows in the capillary, ΔP would decrease from an initial value due to the viscous resistance until it hits the thermoresponsive hydrophobic patch. A sudden increase in the contact angle of liquid with the hydrophobic surface of the valve will lead to significant drop in the driving pressure, ΔP (increasing θ causes $\cos\theta$ to decrease). In addition to the loss of the driving pressure gradient, the liquid–solid contact line is expected to get pinned (Fig. 1(c)) and prevent further advancement of the meniscus.[10]

3. EXPERIMENTAL PROCEDURE

3.1. Fabrication

In order to control the surface wettability for flow regulation, a fabrication strategy which would allow a localized, conformal coating on a non-flat surface needs to be identified. For the dual-scale textured base, hybrid multilayers consisting of poly(allylamine hydrochloride) (PAH), poly(acrylic acid) (PAA) and colloidal silica nanoparticles (average diameter = 22 nm and 7 nm) were used. Based on the electrostatic interactions between the polyelectrolytes and nanoparticles, a layer-by-layer (LBL) deposition technique in combination with photolithography was employed to obtain a localized, conformally-coated patch in a microchannel.

The open area of glass was prepared with adhesive layers of poly(allylamine hydrochloride)(PAH)/poly(styrene sulfonate) (PSS). 3 bilayers of PAH/silica nanoparticles were dip-coated. Then, 2 bilayers of PAH/PAA was applied. PNIPAAm was grafted using 2,2-azobis (2-methylpropionamidine) dichloride (ABMP) and N-(3-dimethlyaminopropyl)-N-ethylcarbodimide (EDC) as an initiator. Finally, perfluorosilane was vapor–deposited on a top layer. The test device was completed after bonding a PDMS cover slab over the microchannel. More detailed fabrication steps were described in Ref. [11].

3.2. Characterization

The surface morphology was characterized using Atomic Force Microscopy (AFM, Pico SPM). AFM images were obtained with a scan ranging from 500 nm to 1 μm in a tapping mode with a force constant of 0.5–9.5 N/m. The scan angle was 0°. The wetting angles were measured with a contact angle goniometer. The pressure in a microfluidic channel with the wettability control surface was measured using a two port differential pressure sensor (PX 2300-2DI, Omega Engineering Inc. Stamford, CT). The measured pressure values are logged by a 4 channel voltage recorder (OM-CP-QUADVOLT, Omega Engineering

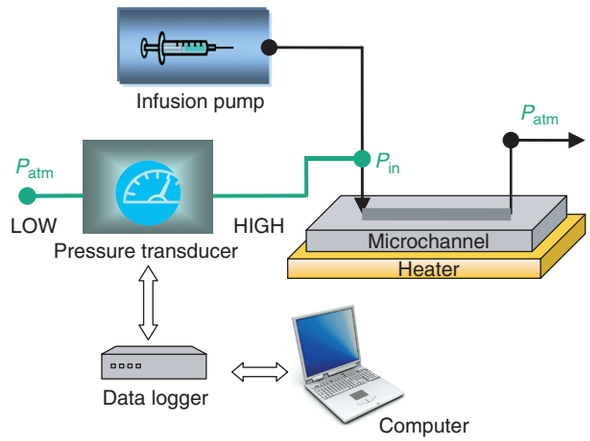

Fig. 2. Schematic illustration of the pressure measurement setup.

Inc., Stamford, CT) at a fixed frequency. The differential pressure drop measured by the sensor is, $\Delta P = P_{in} - P_{atm}$ as given by Eq. (5). Figure 2 illustrates the measurement setup.

4. RESULTS AND DISCUSSION

Figure 3(a) shows a cross-sectional image of a rough multilayered film, on which a small amount of silica nanoparticles are decorated in the initial stage of LBL process. From Figure 3(b), it can be observed that the microscale undulation is mainly introduced by the polyelectrolytes. Figures 3(b) and (c) show that the dual length scale

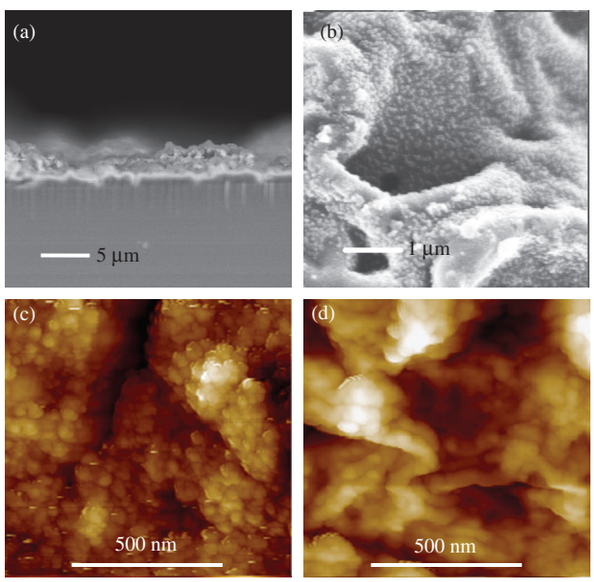

Fig. 3. (a) SEM cross-sectional image of a film on a glass substrate (b) SEM image of rough multilayered film showing microscale undulation (c) AFM image of dual length scale micro-nano textures introduced by PAH/silica multilayers (d) AFM image after PNIPAAm deposition.

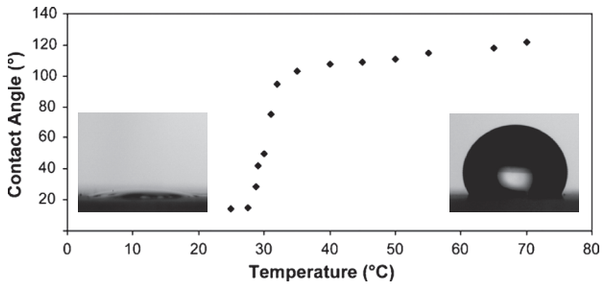

Fig. 4. Water contact angle measured upon the thermoresponsive surface with dual length scale texture as a function of temperature.

textures introduced by PAH/silica hybrid multilayers and preserved even after PNIPAAm deposition, respectively.

The water contact angle measured as a function of temperature is shown in Figure 4. When the surface of the valve changes from hydrophilic ($\theta < 90°$) to hydrophobic ($\theta > 90°$), the capillary pressure changes signs. At room temperature, the valve is in hydrophilic state; therefore the flow is allowed to pass without any obstruction whereas for elevated temperatures ($T > 33°C$) valve attains a gating action.

Figure 5 shows the variation of the differential pressure at various stages of the fluid flowing and halting in the device. The initial pressure build-up is required to overcome the entrance into the device and filling of the inlet reservoir of the microchannel (point A). The pressure differential decreases as soon as the water enters the microfluidic devices as expected, since the water enters the device inlet reservoir which has a larger volume and is made in a hydrophilic glass substrate.

As the water starts to flow in the microchannel under the influence of capillary action (point B), the pressure steadily decreases due to viscous losses until the

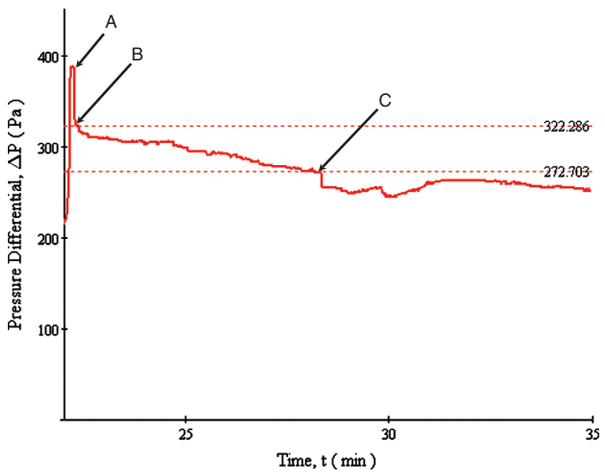

Fig. 5. Variation of a differential pressure as the flow is introduced to the device. The measurement was carried out at $T = 55$ °C at which the thermoresponsive surface is hydrophobic.

water front reaches the thermoresponsive polymer surface. The water stops flowing when it comes in contact with the hydrophobic thermoresponsive polymer (point C in the plot) due to an abrupt change in contact angle.

The second case of surface energy consideration occurs when the water front reaches the glass-PNIPAAm contact line. The switchable thermoresponsive PNIPAAm surface is conformally coated on both the side walls and the floor of the glass microchannel. The flow experiment is carried out at a temperature of 55 °C. At this temperature, the contact angle of a water droplet on the switchable thermoresponsive hydrophobic surface is approximately 114°. Since the water encounters three surfaces (two side walls and the floor) which have a contact angle of 114° and the top PDMS ceiling which has a contact angle of 110°, the water front now experiences overall hydrophobicity.

This can alternatively be explained by the concept of pseudo-hydrophilicity.[10] As the water is flowing due to capillarity in the hydrophilic glass channel, the top view of the advancing meniscus profile is concave (when seen from the gas). When the advancing meniscus encounters the hydrophobic thermo-responsive polymer, the front ends of the concave radius are pinned to the hydrophobic surface. Due to the pinning, the body of water mass which is still on the hydrophilic glass surface is suddenly pulled forward till it encounters the hydrophobic thermoresponsive surface. This sudden forward flow is manifested as a decrease in the pressure differential (point C). The meniscus has to maintain contact with the walls of the microchannel but cannot move forward over the hydrophobic surface and attain a hydrophobic convex shape. It can still be viewed as a static hydrophilic front. This phenomenon is described as pseudo-hydrophilicity.

In theory, the maximum pressure that the thermoresponsive valve can withstand was found to be $\Delta P =$ 356 Pa; however, measurements show an abrupt drop of pressure of a few tens of Pascal when the flow is halted at the valve with a residual pressure of 270 Pa that is with held in the system. The former pressure drop can be attributed to the sudden variation of contact angle between the fluid and the solid surfaces and the latter is a pressure value specific to the device that can change based on the hydraulics of the microchannels. For increasing the maximum pressure, the thermo responsive material can be used with geometry-based passive valve concepts.

5. CONCLUSION

Using a nanostructure embedded thermoresponsive polymer fabricated by a layer-by-layer self-assembly method, a flow regulation function was achieved with a tunable wetting surface. A successful gating action was observed when used in capillary driven flows in a microchannel. Convenient fabrication and implementation of such tunable wetting surfaces with robust performance promises a wide array of engineered surfaces for functional flow regulations.

Acknowledgment: National Science Foundation (EEC-0741508 and ECCS-0901503), USA and Korea Science and Engineering Foundation (WCU Program) for their support.

References and Notes

1. G. Londe, A. Chunder, A. Wesser, L. Zhai, and H. J. Cho, *Sens. Actuators B: Chemical* 132, 431 **(2008)**.
2. J. Xi, J. J. Schmidt, and C. D. Montemagno, *Nat. Mater.* 4, 180 **(2005)**.
3. D. Kuckling, C. D. Vo, and S. E. Wohlrab, *Langmuir* 18, 4263 **(2002)**.
4. G. V. Rama Rao, M. E. Krug, S. Balamurugan, H. Xu, Q. Xu, and G. P. Lopez, *Chemistry of Materials* 14, 5075 **(2002)**.
5. J. Lahann, S. Mitragotri, T.-N. Tran, H. Kaido, J. Sundaram, I. S. Choi, S. Hoffer, G. A. Somorjai, and R. Langer, *Science* 299, 371 **(2003)**.
6. M. Zhou, C. Feng, C. Wu, W. Ma, and L. Cai, *J. Nanosci. Nanotechnol.* 9, 4211 **(2009)**.
7. A. Klamchuen and S. Pratontep, *J. Nanosci. Nanotechnol.* 9, 1509 **(2009)**.
8. S. Taolei, W. Guojie, F. Lin, L. Biqian, M. Yongmei, J. Lei, and Z. Daoben, *Ange. Chem. Int. Ed.* 43, 357 **(2004)**.
9. R. F. Probstein, Physicochemical Hydrodynamics, An Introduction, Butterworths, Boston **(1989)**.
10. J.-W. Choi, A. Puntambekar, C. H. Ahn, S. Kim, and V. Makhijani, *Lab on a Chip* 2, 213 **(2002)**.
11. A. Chunder, K. Etcheverry, G. Londe, H. J. Cho, and L. Zhai, *Colloids Surf. A: Physicochemical and Engineering Aspects* 333, 187 **(2009)**.

Received: 15 November 2009. Accepted: 25 March 2010.